HHS Public Access

Author manuscript

Int J Radiat Oncol Biol Phys. Author manuscript; available in PMC 2021 November 15.

Published in final edited form as:

Int J Radiat Oncol Biol Phys. 2020 November 15; 108(4): 1091–1102. doi:10.1016/j.ijrobp.2020.06.070.

Protons and High-Linear Energy Transfer Radiation Induce Genetically Similar Lymphomas With High Penetrance in a Mouse Model of the Aging Human Hematopoietic System

Rutulkumar Patel, PhD[*], **Luchang Zhang, BS**[†], **Amar Desai, PhD**[†,‡], **Mark J. Hoenerhoff, DVM, PhD**[§], **Lucy H. Kennedy, DVM**[§], **Tomas Radivoyevitch, PhD**[‖], **Chiara La Tessa, PhD**[¶,#], **Stanton L. Gerson, MD**[‡], **Scott M. Welford, PhD**[**,††]

[*]Department of Radiation Oncology, Duke University, Durham, North Carolina;

[†]Department of Medicine, Case Western Reserve University, Cleveland, Ohio;

[‡]Case Comprehensive Cancer Center, Case Western Reserve University, Cleveland, Ohio;

[§]Unit for Laboratory Animal Medicine, University of Michigan, Ann Arbor, Michigan;

[‖]Department of Quantitative Health Sciences, Cleveland Clinic, Cleveland, Ohio;

[¶]University of Trento, Trento, Italy;

[#]Trento Institute for Fundamental Physics and Applications TIFPA-INFN, Trento, Italy;

[**]Sylvester Comprehensive Cancer Center, University of Miami, Miami, Florida;

[††]Department of Radiation Oncology, University of Miami, Miami, Florida

Abstract

Purpose: Humans are exposed to charged particles in different scenarios. The use of protons and high-linear energy transfer (LET) in cancer treatment is steadily growing. In outer space, astronauts will be exposed to a mixed radiation field composed of both protons and heavy ions, in particularly the long-term space missions outside of earth's magnetosphere. Thus, understanding the radiobiology and transforming potential of these types of ionizing radiation are of paramount importance.

Methods and Materials: We examined the effect of 10 or 100 cGy of whole-body doses of protons or ^{28}Si ions on the hematopoietic system of a genetic model of aging based on recent studies that showed selective loss of the MLH1 protein in human hematopoietic stems with age.

Results: We found that *Mlh1* deficient animals are highly prone to develop lymphomas when exposed to either low doses of protons or ^{28}Si ions. The lymphomas that develop are genetically indistinguishable, in spite of different types of damage elicited by low- and high-LET radiation. RNA sequencing analyses reveal similar gene expression patterns, similar numbers of altered

Corresponding author: Scott M. Welford, PhD; scott.welford@med.miami.edu.

The authors declare no conflicts of interest.

Research data are stored in an institutional repository and will be shared upon request to the corresponding author.

Supplementary material for this article can be found https://doi.org/10.1016/j.ijrobp.2020.06.070.

genes, similar numbers of single nucleotide variants and insertions and deletions, and similar activation of known leukemogenic loci.

Conclusions: Although the incidence of malignancy is related to radiation quality, and increased due to loss of *Mlh1*, the phenotype of the tumors is independent of LET.

Introduction

Ionizing radiation (IR) affects biology in several contexts, the most typical being imaging modalities and cancer therapy. The absorption of energy from x-rays or gamma rays at low doses is used to visualize differential tissue densities, but at high doses can be used to cause toxic DNA damage and subsequent cell death. Next-generation cancer therapies are moving toward the use of protons or heavier ions such as carbon nuclei owing to the favorable depth-dose distribution that allows improved sparing of healthy tissue, and in the case of ion therapy, more complex and less reparable DNA damage that leads to improved cell kill. Coincidentally, the use of IR for medical purposes has to be balanced by the risk of cellular transformation that can also occur from damaging DNA. Although many studies have been performed in the whole range of model organisms and humans on the detrimental effects of x-rays and the applications of ions in radiation therapy requires a deeper knowledge of the effects of protons and high-LET radiation on biology.

Future space missions also depend on a greater understanding of radiobiology. Risks associated with human space travel include exposure to space radiation, consisting of a broad spectrum of low-, medium-, and high-LET radiation sources that include galactic cosmic rays (GCR), solar energetic particles, and the Van Allen radiation belts.[1,2] In particular, GCR is composed of low-LET protons (85%) and high-LET nuclei of heavier elements, called HZE (high atomic number Z and energy E) particles.[3] Although the latter contributes to less than 1% of GCR, their physical properties lead to far more detrimental biological effects in living cells. HZE deposit large amounts of energy throughout the track of each particle and thus create secondary ionizations from energetic electrons stripped away from atoms or molecules by the incoming radiation.[3] HZE particles cause more biological damage in living cells compared with conventional x-rays, including chromosomal aberrations and DNA damage that can lead to cancer.[4,5] Several reports, starting from 1985 by the Ullrich group, demonstrated that high-LET radiation exposure in animals leads to increase tumorigenesis compared with low-LET radiation.[6–12] Recent studies investigating mechanisms have shown that high-LET ^{28}Si ions can cause persistent increases in inflammation and immune changes due to activated NF-κB, TNF-α, IL-1β, and IL-6 in mouse bone marrow cells.[13] Furthermore, low- and high-LET radiation exposure also yield differences at epigenetic and gene expression levels.[14,15] What is unclear, however, is whether tumors induced by radiation sources of different LET are distinct, or pose different clinical paradigms; questions that can be addressed most robustly with next generation sequencing technologies.

The hematopoietic system is one of the most sensitive to radiation-induced damage and can have both acute and latent ramifications. Next to the gut, radiation toxicity is most often due to hematopoietic failure at high doses; and radiation-induced leukemias and lymphomas are

the most common early malignancies.[16] Several animal studies have shown that exposure to high-LET simulated-space radiation causes elevated levels of leukemia and lymphomagenesis compared with x-rays.[10,17] Most of these studies irradiated young adult animals to allow longer follow-up periods. Although informative, these studies could not detect the effects of genetic and epigenetic changes that accumulate in hematopoietic stem cells (HSCs) or hematopoietic progenitor cells (HPCs) as a function of age that could affect cancer formation. MLH1 is a major component of the DNA mismatch repair (MMR) pathway, and we recently demonstrated that human stem cells lose MLH1 expression as a result of promoter hypermethylation with age.[18,19] Given that most cancer patients and astronauts are middle-aged or elderly, HSCs with compromised MMR function are thus a better model for ascertaining the effects of ions on hematopoietic malignancy. Therefore, we used *Mlh1* heterozygous mice to represent aging human HSCs and irradiated them with either protons or ^{28}Si ions to gain insight into the frequency and latency of tumorigenesis. We found that exposure to ^{28}Si ions caused a significantly higher level of tumorigenesis with reduced latency compared with protons. There was no evidence of elevated tumor grade. Histologic and immunohistochemistry analyses revealed that the great majority of tumors were indistinguishable lymphomas, particularly a T-cell rich B-cell (TRB) variety, regardless of the radiation source. RNA-sequencing analyses of the tumors demonstrated that gene expression and biological pathways involved in the process of lymphomagenesis were similar between low- and high-LET induced lymphomas, and further that common human leukemogenic loci were similarly activated in the tumors. In summary, therefore, protons and high LET radiation induce identical tumors, but at different incidence rates. The inclusion of MMR deficiency as an aging model significantly increased malignancy.

Methods and Materials

Animals

Mlh1$^{+/-}$ mice (B6.129-Mlh1^{tm1Rak}/NCI) were acquired from the National Cancer Institute Mouse Repository. All animals were bred, genotyped, and maintained for experiments at Case Western Reserve University (CWRU). Institutional Animal Care and Use Committee–approved protocols were followed for designing and implementing all experiments at CWRU and at Brookhaven National Laboratory (BNL). All animals were kept in individually ventilated cages with ad libitum access to food (Laboratory Rodent Diet 5LOD, Laboratory Diet, St Louis, MO) and sterilized water. The animal housing room was maintained on a 12:12h light:dark cycle and constant temperature (72°F ± 2°F). Daily animal health checks were performed by the animal husbandry staff at CWRU.

Particle irradiation

Radiation exposures were performed at the NASA Space Radiation Laboratory of BNL.[20] Twelve-week-old male and female mice were shipped to BNL at least 1 week before irradiation. The animals were divided into groups of ~40 animals to obtain statistical power. On the day of exposure, animals were arranged into an animal pie-shaped holder and irradiated with a 20 × 20 beam of 10 or 100 cGy of 1000 MeV/n protons (LET 0.23 keV/micron) or ^{28}Si 300 MeV/n ions (LET 70 keV/micron) at a dose rate of 5 to 50 cGy/min. Sham-irradiated *Mlh1*$^{+/+}$ and *Mlh1*$^{+/-}$ animals traveled and were treated the same way as

irradiated cohorts. Sham-irradiated animals used in the present study were the same as our previously published study.[21]

Blood analysis

Irradiated and sham-irradiated mice were bled via the submandibular vein at 5-month and 9-month time points post exposure (n = 36–44 mice/treatment group). Collected blood (50–75 μL) was analyzed by HemaVet 950FS auto blood analyzer to measure the distribution of white blood cell, red blood cell, and platelets.

Histopathology and immunohistochemistry

Tumors and abnormal organs were collected at the first sign of morbidity. Mice were terminated using CO_2 chamber as per Institutional Animal Care and Use Committee (IACUC) protocol followed by complete necropsy. All abnormal organs and tumors were fixed in 10% formaldehyde, and a small portion of tumors was also snap-frozen in liquid nitrogen. Tissue processing and hematoxylin and eosin staining were carried out by the Pathology Core at University Hospitals and CWRU, Cleveland, OH. Immunohistochemistry was performed by the In Vivo Animal Core in the Unit for Laboratory Animal Medicine at the University of Michigan, Ann Arbor, MI. Selected lymphoma samples were labeled with B220 (BD Pharmingen # 550286), CD3 (Thermo Fisher # RM9107), and F4/80 (Abd Serotec # MCA497RT) antibodies. Histopathologic analysis was performed by a board-certified veterinary pathologist (M.J.H.) using an Olympus BX43 light microscope.

RNA-sequencing and analysis

Snap-frozen lymphoma samples were used to collect RNA for sequencing and analysis purposes. RNA was extracted using RNeasy Qiagen Mini Kit (Cat #74104), and samples were sent to Novogene Bioinformatics Technology Co., Ltd for additional analysis. All samples were tested for RNA purity via Nanodrop and potential contamination via Agarose gel electrophoresis. Each RNA sample's integrity was further checked via Agilent 2100, and samples with RIN (RNA integrity number) ≥6 were selected for the next step. The construction of cDNA library was performed from RNA samples, and the quality of the library was assessed before Illumina paired-end sequencing. Subsequently, the library preparations were sequenced on Illumina Plateform, and paired-end reads (2×150 bp, 20M reads/sample) were generated at Novogene. Raw data processing and quality assessment, mapping reads to reference genome, gene expression level analysis, and functional analysis of differentially expressed genes were performed by the bioinformatics team at Novogene.

Results

Exposure to ^{28}Si ions caused early and higher incidence of tumorigenesis compared with protons in Mlh1 $^{+/-}$ mice

In the early 1990s, a germline mutation in one of the critical MMR proteins, MLH1, was found to be associated with Lynch syndrome, an autosomal dominant genetic condition associated with a subset of colorectal cancers.[22,23] Throughout the years, studies have shown a strong correlation between loss of *MLH1* and other malignancies, such as glioblastoma, endometrial cancer, lung cancer, and head and neck cancer.[24–27] In fact, MMR defects

measured by microsatellite instability are now found in more than 18 cancer types,[28] and can serve as a genetic predisposition to cancer development.[29] To understand the combined effect of loss of *Mlh1* and low- or high-LET radiation exposure on the hematopoietic system, *Mlh1* wild type and heterozygous mice were irradiated with 10 or 100 cGy of protons or ^{28}Si ions and blood samples were collected at 5 and 9 months postexposure to detect any signs of hematopoietic abnormality. The doses were chosen because they are both well in the range of expected exposure levels on Mars missions, and because prior studies of tumorigenesis in mice indicate that we would be able to see sensitization effects.[10] Red blood cell and platelets were found to be significantly elevated after ^{28}Si compared with protons at 5 months ($P < .0001$) but absent at 9 months (Fig. E1A–1D). In contrast, white blood cells were significantly decreased after 10 cGy of ^{28}Si compared with 10 cGy of protons at 5 months ($P < .0001$), but again unchanged at 9 months (Fig. E1E and E1F). Collectively, these data suggest that high-LET ^{28}Si ion irradiation had an effect on HSC differentiation at the 5-month time point, but not at the 9-month time point, suggesting that primitive HSCs are capable of whole blood reconstitution throughout the lifespan of an organism after the initial assault. However, *Mlh1* status of mice did not play a role in HSC differentiation at any time points, and we have previously demonstrated that *Mlh1* deficiency does not affect short- and long-term HSC functions.[30]

During the follow-up period of irradiated mice, we killed any mice with visible signs of distress, and only mice with tumors were included for the remainder of the analysis. Tumor-free survival of $Mlh1^{+/+}$ mice after irradiation did not show a significant increase in tumorigenesis compared with sham irradiated mice (Fig. 1B, P = not significant). However, tumor-free survival of $Mlh1^{+/-}$ mice after 10 cGy or 100 cGy of protons or ^{28}Si irradiation showed a significant increase in tumorigenesis compared with the sham irradiated $Mlh1^{+/-}$ mice (Fig. 1C, $P < .0001$). In addition, tumorigenesis was significantly elevated after 100 cGy ^{28}Si compared with 100 cGy protons ($P = .0001$), showing a clear effect of high-LET radiation on tumorigenic potential. We found 32% of the sham irradiated mice formed spontaneous tumors, although 60% of the 100 cGy proton irradiated mice and 96% of the 100 cGy ^{28}Si mice developed tumors (Fig. 1E). Furthermore, we noted the latency of tumor occurrence by comparing the time for $Mlh1^{+/-}$ cohorts to reach 70% survival after sham, 100 cGy of protons, or 100 cGy of ^{28}Si. The comparison showed that 70% survival for the cohort irradiated with ^{28}Si was significantly lower (370 days) compared with cohort irradiated with protons (439 days) or sham-irradiated cohorts (513 days; Fig. 1D). Collectively, our data suggest that high-LET causes early and higher incidence of tumorigenesis compared with low-LET radiation in *Mlh1* heterozygous, mice.

Lymphoma was found as a primary tumor type, regardless of Mlh1 status or type of radiation

During necropsy, any visible abnormal mass or tumor was collected and immediately snap-frozen or fixed in 10% formaldehyde solution for later analysis. Lymphomas are among the most prevalent tumor types in many laboratory strains of mice, including C57BL/6.[31] Therefore, we performed a histologic analysis to identify the tumor type induced by radiation. We found lymphomas as a primary tumor type most frequently occurring in mesenteric lymph nodes, and less frequently occurring in organs such as the spleen, liver,

and intestine (Fig. 2C–2F). In fact, the percentage distribution analysis of different tumor types showed that loss of *Mlh1* accelerates lymphomagenesis, leading to almost double the incidence of lymphomas in $Mlh1^{+/-}$ cohorts compared with $Mlh1^{+/+}$ cohorts (Fig. 2G and 2H). In addition, we also found hepatocellular carcinomas (Fig. 2A) and radiation-induced histiocytic sarcomas (Fig. 2B) as common tumor types. However, we did not find a significant difference in tumor type distribution caused by ^{1}H ion versus ^{28}Si ion exposure, regardless of *Mlh1* status of the mice (Table E1). The data suggest that loss of *Mlh1* plus radiation expedites lymphomagenesis, regardless of the type of radiation received.

Although analyzing tumor incidence data, we observed that $Mlh1^{+/-}$ mice showed a significantly higher incidence of multiple lymphomas per mouse compared with $Mlh1^{+/+}$ mice (Fig. 2I, $P = .05$). However, radiation exposure did not cause a further increase in the incidence of multiple lymphomas, suggesting that *Mlh1* deficiency, but not irradiation, was a primary cause of multiple lymphomas incidence. Additional analysis of lymphomas by immunohistochemistry revealed that the majority of the lymphomas could be characterized as B-cell lymphomas with a high level of infiltrating T-cells (Fig. E2A–2C, Table E2). *Mlh1* status or radiation type did not change the prevalence of these T-cell rich B-cell (TRB) lymphomas across different cohorts (Fig. E2D and E2E). Together, we found that loss of *Mlh1*, but not the type of radiation exposure, was strongly associated with lymphomagenesis, and TRB lymphomas were the most common subtype of lymphomas found.

Gene expression and mutational analysis of TRB lymphomas revealed no distinctions between ^{1}H ion versus ^{28}Si ion exposure

To elucidate molecular pathways that govern the process of lymphomagenesis, we performed RNA-sequencing analysis of TRB lymphomas collected from $Mlh1^{+/+}$ and $Mlh1^{+/-}$ mice exposed to sham, ^{1}H ion, or ^{28}Si ion IR. At a level of gene expression, we found over 10,000 genes were differentially expressed compared with control lymph nodes (age-matched sham-irradiated lymph nodes) with an adjusted *P* value threshold of .05. We observed no distinct gene expression pattern or clustering arising due to loss of *Mlh1* or radiation exposure induced lymphomas, as shown in a heatmap in Fig. 3A. However, hierarchical cluster analysis revealed clear grouping of age-matched lymph nodes either coming from $Mlh1^{+/+}$ or $Mlh1^{+/-}$ mice (Fig. 3A, left side). Looking at differentially expressed genes, we were unable to detect any significant changes in the number of genes downregulated due to treatment conditions (Fig. 3B). Similarly, we observed no differences in the number of upregulated genes between different treatment conditions, except a slightly lower number of genes were found to be upregulated in ^{28}Si ion induced $Mlh1^{+/-}$ lymphomas compared with ^{28}Si ion induced $Mlh1^{+/+}$ lymphomas (Fig. 3C, $P = .05$). In addition, we noticed that a higher number of genes were downregulated compared with upregulated in each treatment group with higher significant differences (greater −log10 [corrected *P* value]), as shown in volcano plots (Fig. E3). Furthermore, we analyzed RNA-sequencing data to determine how *Mlh1* status or radiation quality factor affects the number of single nucleotide variants (SNVs) and insertions and deletions (INDELs) in TRB lymphomas. Surprisingly, the analysis revealed no further increase in SNVs and INDELs due to low- or high-LET radiation exposure, regardless of *Mlh1* status (Fig. 3D and 3E). In

contrast, Loss of *Mlh1* was clearly associated with significantly elevated levels of SNVs and INDELs, regardless of the type of radiation exposure (Fig. 3D and 3E). Collectively, RNA-sequencing analysis was unable to detect any gross differences at gene expression and mutational/deletion levels due to ^{1}H ion versus ^{28}Si ion induced lymphomas.

Similar oncogenic signaling pathways were involved across all cohorts of TRB lymphomas

We sought to determine whether any distinct biological pathways or genes were involved in the process of lymphomagenesis. We compiled a list of differentially expressed genes from each cohort of TRB lymphomas and looked at the number of common genes present among all cohorts. Surprisingly, we discovered that ~50% of differentially expressed genes were shared among all cohorts of TRB lymphomas (Fig. 4A). In fact, we found that ~70% and ~60% of mutual genes were appeared between protons versus ^{28}Si and *Mlh1*$^{+/+}$ versus *Mlh1*$^{+/-}$ lymphomas, respectively. To gain insight into biological functions pertaining to each condition, we performed gene ontology analysis on differentially expressed genes to identify which biological functions or pathways were preferentially governed the process of lymphomagenesis. We looked at differentially expressed genes via the KEGG (Kyoto Encyclopedia of Genes and Genomes) database and found no distinct pathways altered in any cohorts of TRB lymphomas (Fig. 4B–4F). We discovered that alteration of mismatch repair pathway was one of the top hits that appeared in every cohort of TRB lymphomas, including *Mlh1*$^{+/+}$ cohorts, suggesting the importance of MMR pathway defect in tumorigenesis.

Furthermore, we used NanoString Technologies' mouse cancer and immune pathway database to identify unique, well-defined cancer pathways in each cohort of TRB lymphomas. Based on functional gene categorization, we separated the number of genes present in each category of cancer pathways and asked the question of whether *Mlh1* status or irradiation quality factor plays a discriminating role in the process of lymphomagenesis. Again, we noticed that almost an equal number of carcinogenic loci were present in each category of well-defined cancer pathways, regardless of *Mlh1* status or type of radiation exposure (Fig. 5A and 5B, P = ns). The analysis also revealed that roughly 37% of carcinogenic loci were present in each cohort of TRB lymphomas (Fig. 5C). In contrast, we found very few carcinogenic loci differentially expressed due to either protons (Tmem173, Pdcd1, Ccl5, Zbp1, Ets2, Il1r2, Spp1, Col6a6, and Cd79b) or ^{28}Si ion (Colec12 and Ptprc) induced TRB lymphomas (Table E3, available https://doi.org/10.1016/j.ijrobp.2020.06.070). Moreover, we generated a heatmap by using expression values of carcinogenic loci that were 1.5-fold differentially expressed in either direction with an adjusted P value of less than .05. Hierarchical clustering analysis revealed no clear grouping of TRB lymphomas based on *Mlh1* status or type of radiation exposure (Fig. 5D). Collectively, RNA-sequencing analysis revealed that all cohorts of TRB lymphomas were similar at the gene expression level, suggesting that even though we observed a significantly higher incidence of lymphomas post ^{28}Si ion compared with protons, the process of lymphomagenesis was similar to post low- versus high-LET exposure.

Discussion

The effect of protons and heavy ions is becoming more relevant to human health, both as we progress to novel radiation therapy technologies, and prepare for deep space missions for astronauts. In the present study, we investigated the leukemogenic and lymphomagenic process in an aging model of human HSCs in mice. It was not surprising to see that high-LET ^{28}Si radiation in an MMR deficient model caused increased malignancy, as this has been previously documented by our group using ^{56}Fe particle exposure.[21] However, the observation that protons and ^{28}Si particle exposure produced phenotypically identical tumors could have implications for patients undergoing proton radiation therapy and astronauts in an outer space radiation environment.

Although heavy ions comprise a small fraction of the galactic cosmic radiation, many ground-based studies, including our previous studies, have revealed that heavy ion exposure in animals causes a variety of adverse health effects. Our present study shows that ^{28}Si ion exposure in *Mlh1* deficient mice significantly increases the incidence of lymphomas compared with protons exposure. In fact, roughly 95% of *Mlh1*$^{+/-}$ mice exposed to 100 cGy ^{28}Si ion developed tumorigenesis, which is higher than the100 cGy proton exposure induced tumorigenesis, and higher than previously reported malignancy caused by ^{56}Fe exposure.[21] Microdosimetric techniques have revealed that roughly 32 cells are hit by low-LET delta-rays for each cell traversed by high-LET ^{56}Fe particle.[32] ^{28}Si ions will yield a higher number of secondary electrons than protons, which will hit the surrounding cells, causing additional damage. In addition, LET directly correlates with RBE (relative biological effectiveness) up to a point, after which cell killing overtakes cell transformation. ^{28}Si ions with an energy of 300 MeV/n have a LET of 70 keV/micron, which is well below the LET required to reach the cell overkill point (~200 keV/μm) and therefore could lead to increased cell transformation leading to higher tumorigenesis.[33] Furthermore, heavy ions produce more complex DNA damage and result in increased chromosomal aberrations than low-LET radiation, which is often fatal to cells. Thus, simply by consideration of different mechanisms of DNA damage in cells, one might predict that the tumorigenesis process would be unique between low- and high-LET radiation exposure.

In-depth RNA-sequencing analysis, however, revealed that lymphomagenesis was not changed by the type of radiation exposure. Functional analysis of differentially expressed genes revealed that metabolic pathways were among the top 20 pathways enriched only in irradiated TRB lymphoma cohorts, but not in the sham irradiated cohort. Metabolic reprograming is considered one of the hallmarks of cancer, and many studies have revealed that these changes promote the development and progression of cancer as well as play a crucial role in radiation response.[34,35] In fact, we found downregulation of *Apc* and *Sirt4* in all cohorts of irradiated TRB lymphoma, and several studies have shown a link between loss of *APC* and *SIRT4* driving the metabolic reprogramming in cancer.[36,37] In addition, we found that the mismatch repair pathway was among the top altered pathways in all cohorts of TRB lymphomas, regardless of *Mlh1* status. However, almost all mismatch repair genes were upregulated in all cohorts of TRB lymphomas, except *Mlh1* expression was downregulated in heterozygous cohorts, suggesting the importance of mismatch repair pathway in highly proliferative state of cancer cells. We also looked at well-defined

oncogenes and found that oncogenes, such as *Myc, Nras, Mdm2, Pim1, Kit, Atf1, Raf1*, and *Hmga1* were significantly overexpressed in all cohorts of TRB lymphomas. Furthermore, we have previously shown that *Mlh1* deficient mouse lymphomas resemble human leukemia, so we looked at the expression level of well-defined human leukemia genes in TRB lymphomas induced by protons versus silicon exposure. We found one human leukemia gene (*BCL7A*) was differentially expressed only in ^{28}Si ion induced lymphomas, and 3 human leukemia genes (*CCL5, KCNE4*, and *CD79B*) were differentially expressed only in proton induced lymphomas. Collectively, our data suggest that low- and high-LET IR induced lymphomas were similar at the gene expression level, even though we detected significantly higher and earlier incidence caused by ^{28}Si ion IR.

The possibility does exist that the types of lymphoma that occurred were predisposed by the use of the *Mlh1* mouse. As in Lynch syndrome, MMR genes are generally considered caretaker genes, that when lost, lead to increase genomic instability due to reduced fidelity of DNA repair. Thus the genetic background of the animals may have a more dominant effect than the radiation type. On the other hand, the use of the *Mlh1* mutant is directly relevant to aging hematopoiesis, wherein MLH1 protein is commonly lost. Thus for both patients and astronauts, the differing LET radiation sources will likely have to interact with MMR deficient cells, and the observations here suggest that tumorigenesis is more homogeneous than what may have been predicted from the known mechanisms of damage as they depend on LET. It is also remarkable that the wild type animals showed no increase in tumorigenesis after exposure to the more potent high LET species. Although somewhat in contrast to what others have reported,[7,8,38] mouse strain likely plays a role given that the C57bl6 is more radio-resistant compared with others.

To our knowledge, this is the first study to reveal that low- and high-LET radiation exposure in mice triggers similar genetic alterations leading to lymphomagenesis. We showed that loss of a single gene (*Mlh1*), which occurs in aging human HSCs, caused a significantly greater incidence of lymphomagenesis after sham-, low-, or high-LET radiation exposure, without affecting HSC functions. However, the results should be interpreted carefully, as the aging of the hematopoietic system is a complex process governed by intrinsic and extrinsic alterations. In fact, a recent study has shown a strong correlation between downregulation of human HSC genes (*FLT3, BANK1, ITGA4*, and *HIF1α*) and processes such as lymphoid activation, differentiation, and tissue remodeling.[39] To appreciate the effect of space radiation on the hematopoietic system of astronauts requires a better understanding of aging human HSCs, in particular lineage-affiliated gene expression patterns and epigenetic alteration leading to change in HSC pool. Therefore, future studies should focus on using more relevant mouse models that represent aging human HSC phenotypes driven by specific gene alterations. Notably, we found that high LET radiation demonstrated a dose effect and protons did not. A primary difference between high LET and low LET radiation is sparsely ionizing versus densely ionizing nature. To hit as many cells with high LET radiation, a greater dose is needed; however, due to the track structure, high LET radiation deposits more energy within each cell it hits. Thus, there is a balance between DNA damage that leads to transformation with DNA damage that results in cell death. The data could be interpreted to mean that transformation needs sufficient cells to be hit, but after that, increased damage means increased transformation.

Ground-based space radiation simulation has had limitations in replicating cosmic radiation, but recent advances in physics have made it possible to expose animals or samples to mixed-beams (composed of multiple ion species) at low doses and rates to closely mimic what happens in space. Equally important is the further investigation of the types of radiation that are becoming more common-place in clinical practice (ie, carbon therapy, which also has significantly higher LETs than both photons and protons). The overall significance of this work is an assessment of the risk of secondary malignancy in patients (or primary malignancy in astronauts) after exposure to high LET radiation when considering genetic predispositions that affect aging cancer and astronaut populations. Loss of MMR is common in these groups, and here we modeled MMR loss and radiation exposure. Additional studies will be needed to more accurately predict the risks moving forward, with a particular emphasis on age-appropriate genetic models that may go beyond MMR. Nonetheless, the data here argue that incidence of transformation depends on LET more so than the type of transformation.

Supplementary Material

Refer to Web version on PubMed Central for supplementary material.

Acknowledgments—

We are grateful Adam Rusek, Peter Guida, and others at NASA Space Radiation Laboratory who participated in this project. We thank the core facilities of the University of Michigan, and the Case Comprehensive Cancer Center.

This work was funded by NASA (NNX14AC95G) and the Case Comprehensive Cancer Center (5P30 CA043703).

References

1. Cucinotta FA, Schimmerling W, Wilson JW, et al. Space radiation cancer risks and uncertainties for Mars missions. Radiat Res 2001; 156(5 pt 2):682–688. [PubMed: 11604093]
2. Schimmerling W, Cucinotta FA, Wilson JW. Radiation risk and human space exploration. Adv Space Res 2003;31:27–34. [PubMed: 12577903]
3. Heinrich W, Roesler S, Schraube H. Physics of cosmic radiation fields. Radiat Prot Dosimetry 1999;86:253–258. [PubMed: 11543393]
4. Carrano AV. Induction of chromosomal aberrations in human lymphocytes by x rays and fission neutrons: Dependence on cell cycle stage. Radiat Res 1975;63:403–421. [PubMed: 1162030]
5. Leatherbarrow EL, Harper JV, Cucinotta FA, O'Neill P. Induction and quantification of gamma-H2AX foci following low and high LET-irradiation. Int J Radiat Biol 2006;82:111–118. [PubMed: 16546909]
6. Fry RJ, Powers-Risius P, Alpen EL, Ainsworth EJ. High-LET radiation carcinogenesis. Radiat Res Suppl 1985;8:S188–S195. [PubMed: 3867083]
7. Alpen EL, Powers-Risius P, Curtis SB, DeGuzman R. Tumorigenic potential of high-Z, high-LET charged-particle radiations. Radiat Res 1993;136:382–391. [PubMed: 8278580]
8. Dicello JF, Christian A, Cucinotta FA, et al. In vivo mammary tumourigenesis in the Sprague-Dawley rat and microdosimetric correlates. Phys Med Biol 2004;49:3817–3830. [PubMed: 15446807]
9. Weil MM, Bedford JS, Bielefeldt-Ohmann H, et al. Incidence of acute myeloid leukemia and hepatocellular carcinoma in mice irradiated with 1 GeV/nucleon (56)Fe ions. Radiat Res 2009;172:213–219. [PubMed: 19630525]

10. Weil MM, Ray FA, Genik PC, et al. Effects of 28Si ions, 56Fe ions, and protons on the induction of murine acute myeloid leukemia and hepatocellular carcinoma. PloS One 2014;9:e104819. [PubMed: 25126721]
11. Grahn D, Lombard LS, Carnes BA. The comparative tumorigenic effects of fission neutrons and cobalt-60 gamma rays in the B6CF1 mouse. Radiat Res 1992;129:19–36. [PubMed: 1728054]
12. Trani D, Datta K, Doiron K, Kallakury B, Fornace AJ Jr. Enhanced intestinal tumor multiplicity and grade in vivo after HZE exposure: Mouse models for space radiation risk estimates. Radiat Environ Biophys 2010;49:389–396. [PubMed: 20490531]
13. Tungjai M, Whorton EB, Rithidech KN. Persistence of apoptosis and inflammatory responses in the heart and bone marrow of mice following whole-body exposure to (2)(8)Silicon ((2)(8)Si) ions. Radiat Environ Biophys 2013;52:339–350. [PubMed: 23756637]
14. Broustas CG, Xu Y, Harken AD, Garty G, Amundson SA. Comparison of gene expression response to neutron and x-ray irradiation using mouse blood. BMC Genomics 2017;18:2. [PubMed: 28049433]
15. Aravindan N, Aravindan S, Manickam K, Natarajan M. High energy particle radiation-associated oncogenic transformation in normal mice: Insight into the connection between activation of oncotargets and oncogene addiction. Sci Rep 2016;6:37623. [PubMed: 27876887]
16. Little MP. Cancer and non-cancer effects in Japanese atomic bomb survivors. J Radiol Prot 2009;29(2A):A43–A59. [PubMed: 19454804]
17. Miousse IR, Shao L, Chang J, et al. Exposure to low-dose (56)Fe-ion radiation induces long-term epigenetic alterations in mouse bone marrow hematopoietic progenitor and stem cells. Radiat Res 2014;182:92–101. [PubMed: 24960414]
18. Kenyon J, Fu P, Lingas K, et al. Humans accumulate microsatellite instability with acquired loss of MLH1 protein in hematopoietic stem and progenitor cells as a function of age. Blood 2012;120:3229–3236. [PubMed: 22740444]
19. Kenyon J, Nickel-Meester G, Qing Y, et al. Epigenetic loss of MLH1 expression in normal human hematopoietic stem cell clones is defined by the promoter CpG methylation pattern observed by high-throughput methylation specific sequencing. Int J Stem Cell Res Ther 2016;3:031. [PubMed: 27570841]
20. La Tessa C, Sivertz M, Chiang IH, Lowenstein D, Rusek A. Overview of the NASA space radiation laboratory. Life Sci Space Res (Amst) 2016;11:18–23. [PubMed: 27993189]
21. Patel R, Zhang L, Desai A, et al. Mlh1 deficiency increases the risk of hematopoietic malignancy after simulated space radiation exposure. Leukemia 2019;33:1135–1147. [PubMed: 30275527]
22. Bronner CE, Baker SM, Morrison PT, et al. Mutation in the DNA mismatch repair gene homologue hMLH1 is associated with hereditary non-polyposis colon cancer. Nature 1994;368:258–261. [PubMed: 8145827]
23. Papadopoulos N, Nicolaides NC, Wei YF, et al. Mutation of a mutL homolog in hereditary colon cancer. Science 1994;263:1625–1629. [PubMed: 8128251]
24. Cosgrove CM, Cohn DE, Hampel H, et al. Epigenetic silencing of MLH1 in endometrial cancers is associated with larger tumor volume, increased rate of lymph node positivity and reduced recurrence-free survival. Gynecol Oncol 2017;146:588–595. [PubMed: 28709704]
25. Stark AM, Doukas A, Hugo HH, et al. Expression of DNA mismatch repair proteins MLH1, MSH2, and MSH6 in recurrent glioblastoma. Neurol Res 2015;37:95–105. [PubMed: 24995467]
26. Gutierrez VF, Marcos CA, Llorente JL, et al. Genetic profile of second primary tumors and recurrences in head and neck squamous cell carcinomas. Head Neck 2012;34:830–839. [PubMed: 22127891]
27. Ma Y, Chen Y, Petersen I. Expression and promoter DNA methylation of MLH1 in colorectal cancer and lung cancer. Pathol Res Pract 2017; 213:333–338. [PubMed: 28214209]
28. Hause RJ, Pritchard CC, Shendure J, Salipante SJ. Classification and characterization of microsatellite instability across 18 cancer types. Nat Med 2016;22:1342–1350. [PubMed: 27694933]
29. van Roon EH, van Puijenbroek M, Middeldorp A, et al. Early onset MSI-H colon cancer with MLH1 promoter methylation, is there a genetic predisposition? BMC Cancer 2010;10:180. [PubMed: 20444249]

30. Patel R, Qing Y, Kennedy L, et al. MMR deficiency does not sensitize or compromise the function of hematopoietic stem cells to low and high LET radiation. Stem Cells Transl Med 2018;7:513–520. [PubMed: 29656536]
31. Haines DC, Chattopadhyay S, Ward JM. Pathology of aging B6;129 mice. Toxicol Pathol 2001;29:653–661. [PubMed: 11794381]
32. Brooks A, Bao S, Rithidech K, Couch LA, Braby LA. Relative effectiveness of HZE iron-56 particles for the induction of cytogenetic damage in vivo. Radiat Res 2001;155:353–359. [PubMed: 11175671]
33. Mehnati P, Morimoto S, Yatagai F, et al. Exploration of "over kill effect" of high-LET Ar- and Fe-ions by evaluating the fraction of non-hit cell and interphase death. J Radiat Res 2005;46:343–350. [PubMed: 16210791]
34. Pitroda SP, Wakim BT, Sood RF, et al. STAT1-dependent expression of energy metabolic pathways links tumour growth and radioresistance to the Warburg effect. BMC Med 2009;7:68. [PubMed: 19891767]
35. Yoshida GJ. Metabolic reprogramming: The emerging concept and associated therapeutic strategies. J Exp Clin Cancer Res 2015;34: 111. [PubMed: 26445347]
36. Wang L, Li JJ, Guo LY, et al. Molecular link between glucose and glutamine consumption in cancer cells mediated by CtBP and SIRT4. Oncogenesis 2018;7:26. [PubMed: 29540733]
37. Liu Z, Xiao Y, Zhou Z, et al. Extensive metabolic disorders are present in APC(min) tumorigenesis mice. Mol Cell Endocrinol 2016;427:57–64. [PubMed: 26948948]
38. Bielefeldt-Ohmann H, Genik PC, Fallgren CM, Ullrich RL, Weil MM. Animal studies of charged particle-induced carcinogenesis. Health Phys 2012;103:568–576. [PubMed: 23032886]
39. Rundberg Nilsson A, Soneji S, Adolfsson S, Bryder D, Pronk CJ. Human and murine hematopoietic stem cell aging is associated with functional impairments and intrinsic megakaryocytic/erythroid bias. PloS One 2016;11:e0158369. [PubMed: 27368054]

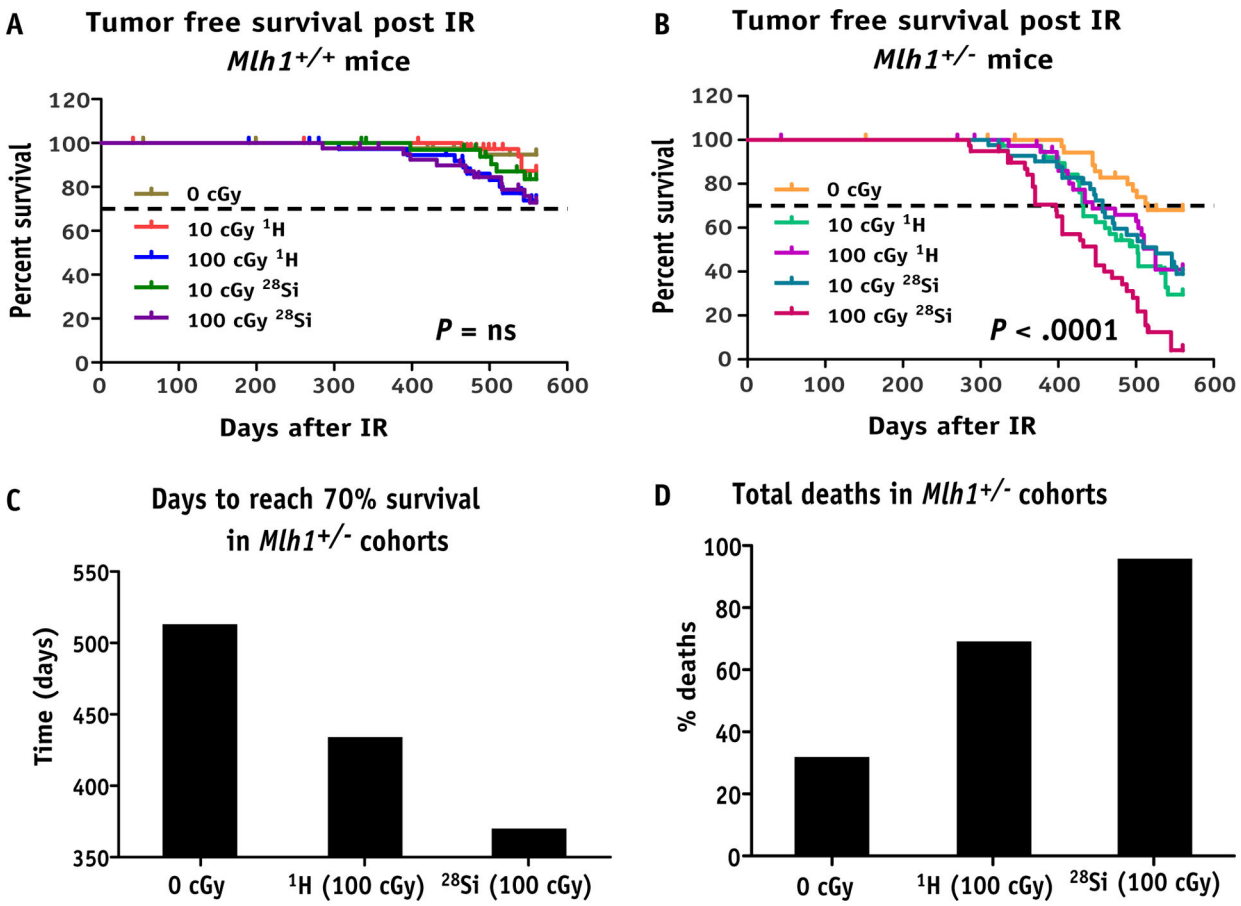

Fig. 1.

Long-term tumorigenesis assay post irradiation. (A) Schematic representation of assay design. (B) Kaplan-Meier plot represents tumor-free survival of *Mlh1*$^{+/+}$ mice post 10 or 100 cGy of ^{1}H or ^{28}Si ion irradiation (n = 36–44, number of *Mlh1*$^{+/+}$ mice used for each radiation exposure group). (C) Kaplan-Meier plot represents tumor-free survival of *Mlh1*$^{+/-}$ mice post 10 or 100 cGy of ^{1}H or ^{28}Si ion irradiation (n = 36–42, number of *Mlh1*$^{+/-}$ mice used for each radiation exposure group). (D) Bar graph represents the number of days to reach 70% survival in each *Mlh1*$^{+/-}$ cohort irradiated with sham, 100 cGy of ^{1}H ions, or 100 cGy of ^{28}Si ions. (E) Bar graph represents the percentage of death occurred in each *Mlh1*$^{+/-}$ cohort irradiated with sham, 100 cGy ^{1}H ions, or 100 cGy ^{28}Si ions. *P* values in each Kaplan-Meier plot were determined by log-rank (Mantel-Cox) test. *Abbreviations*: IR = ionizing radiation; ns = nonsignificant.

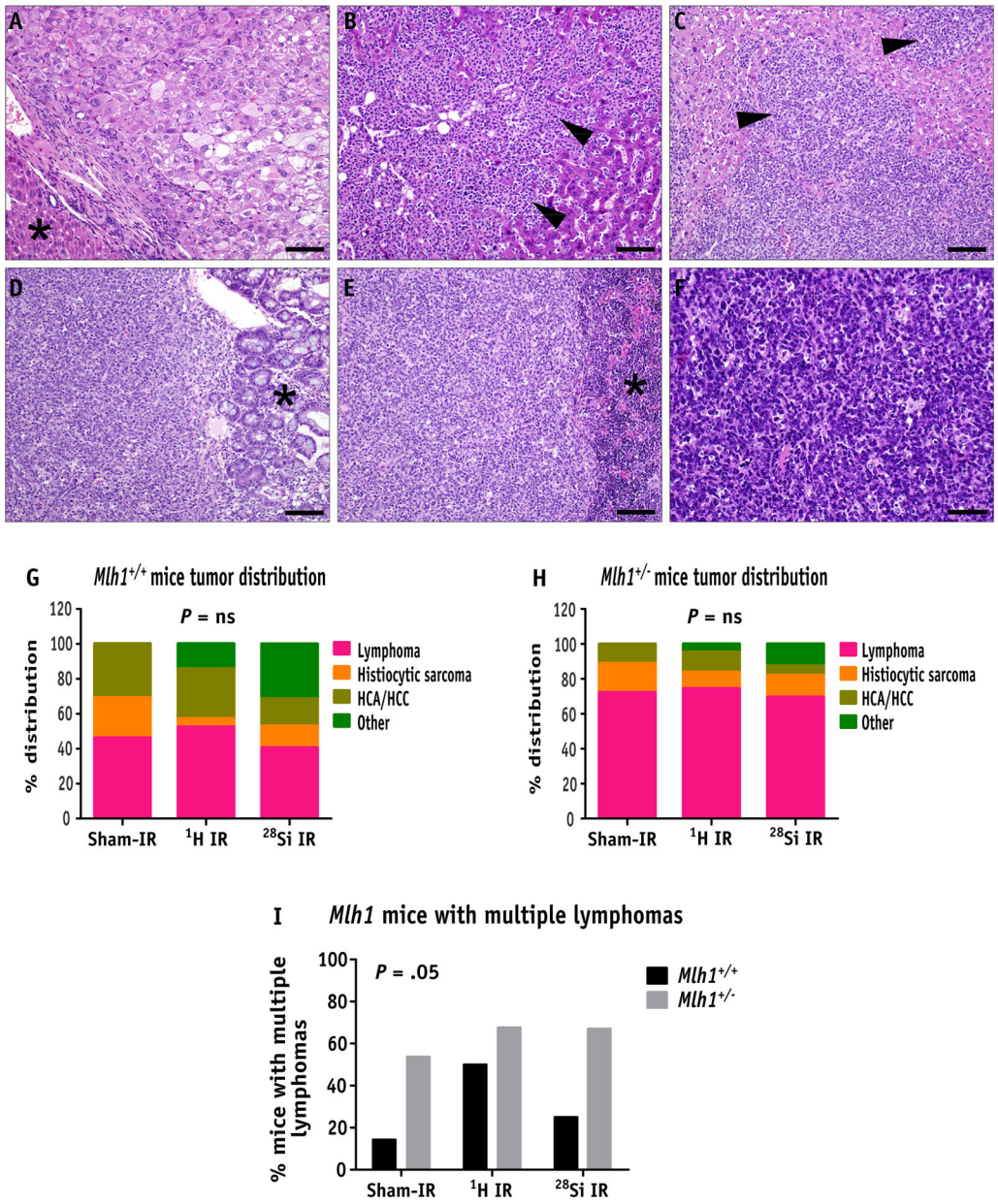

Fig. 2.

Hematoxylin and eosin analysis of tumors obtained from *Mlh1*$^{+/+}$ and *Mlh1*$^{+/-}$ mice. (A) Primary hepatocellular carcinoma composed of solid plates and lobules of poorly differentiated hepatocytes (asterisk denotes normal liver, bar = 50um). (B) Histiocytic sarcoma in the liver, composed of infiltrative sheets of pleomorphic round cells effacing normal hepatic parenchyma (arrowheads, bar = 50um). (C) Lymphoma in the liver, composed of sheets of neoplastic lymphocytes (arrowheads) infiltrating and effacing normal hepatic parenchyma (arrowheads, bar = 50um). (D) GALT lymphoma is expanding the submucosa of the small intestine and infiltrating the overlying intestinal mucosa (asterisk denotes normal mucosa, bar = 50um). (E) Lymphoma effacing the spleen (asterisk denotes normal spleen, bar = 50um) and (F) mesenteric lymph node (bar = 20um), composed of

sheets of atypical lymphocytes. (G) Percent distribution of types of tumors arising in *Mlh1*$^{+/+}$ and (H) *Mlh1*$^{+/-}$ mice post sham, ^{1}H ion, or ^{28}Si ion irradiation. (I) The bar graph represents the percentage of mice with multiple lymphomas in *Mlh1*$^{+/+}$ and *Mlh1*$^{+/-}$ cohorts post radiation exposure. Histopathology was performed on 13 to 32 tumors of *Mlh1*$^{+/+}$ origin and 18 to 56 tumors of *Mlh1*$^{+/-}$ origin. Tumor distribution was analyzed by the χ^2 test, and multiple lymphoma incidence was analyzed by 2-way analysis of variance. *Abbreviation*: GALT = gut associated lymphoid tissue; HCA = hepatocellular adenoma; HCC = hepatocellular carcinoma; ns = nonsignificant.

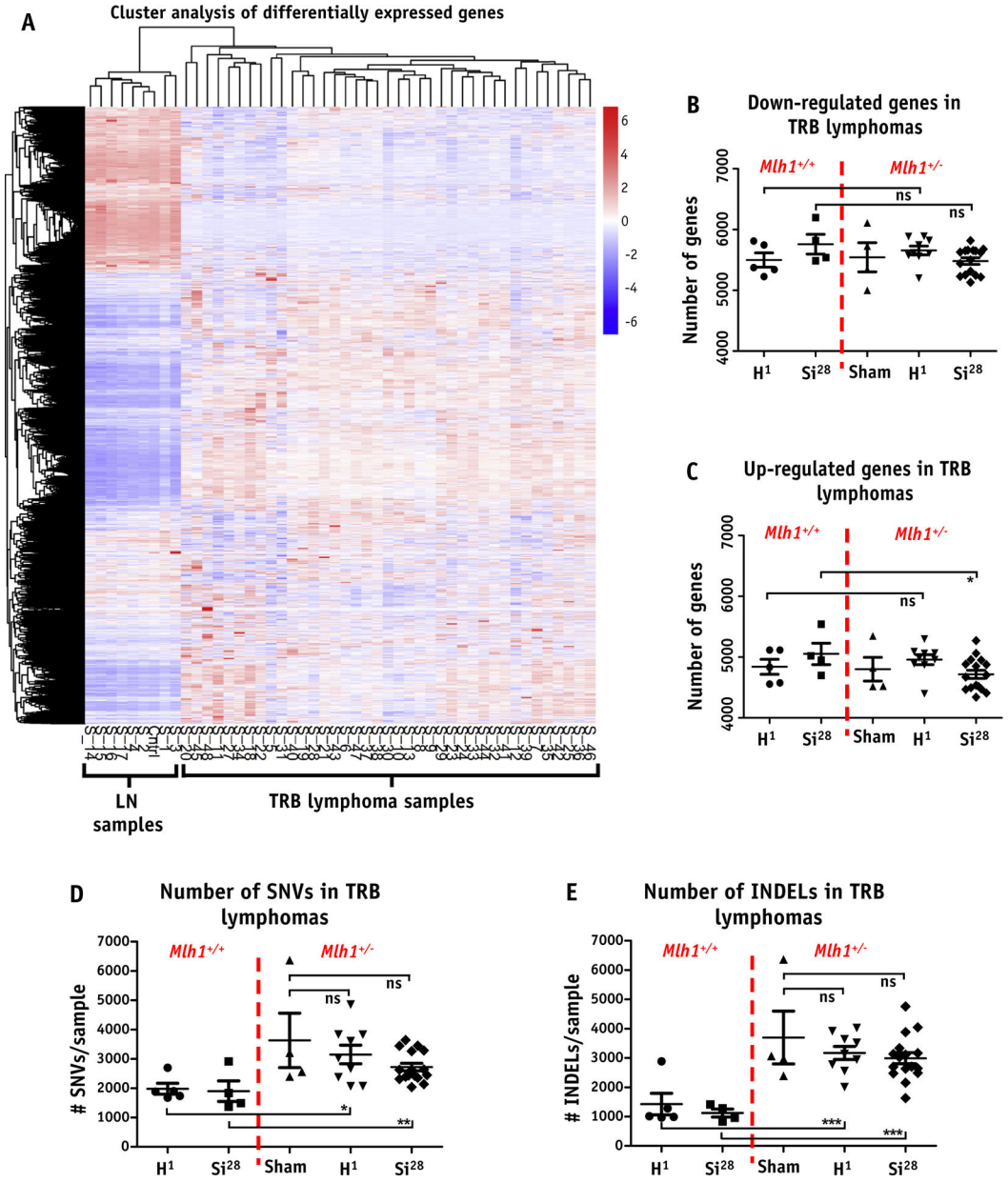

Fig. 3.

RNA sequencing analysis of T-cell rich B-cell (TRB) lymphomas. (A) Heatmap represents gene expression level of each TRB lymphoma arising from sham (n = 4, *Mlh1*$^{+/-}$), ^{1}H ion IR (n = 5 and 9 for *Mlh1*$^{+/+}$ and *Mlh1*$^{+/-}$, respectively), or ^{28}Si ion IR (n = 4 and 16 for *Mlh1*$^{+/+}$ and *Mlh1*$^{+/-}$, respectively) compared with age-matched normal lymph node (n = 4 and 4 for *Mlh1*$^{+/+}$ and *Mlh1*$^{+/-}$, respectively) in the form of hierarchical clustering. Number of genes (B) downregulated, and (C) upregulated, in each TRB lymphoma arising from either *Mlh1*$^{+/+}$ or *Mlh1*$^{+/-}$ mice post sham, ^{1}H ion, or ^{28}Si ion irradiation. (D) Number of single nucleotide variants and TRB lymphoma. (E) Number of insertions and deletions and TRB lymphoma in each cohort of *Mlh1*$^{+/+}$ and *Mlh1*$^{+/-}$ mice post sham, ^{1}H ion, or ^{28}Si ion irradiation. *P* values were determined by unpaired *t* tests;) = $P < .05$,)) = $P < .01$,))) = *P*

< .001. *Abbreviations*: INDEL = insertions and deletions; ns = nonsignificant; SNV = single nucleotide variants; TRB = T-cell rich B-cell.

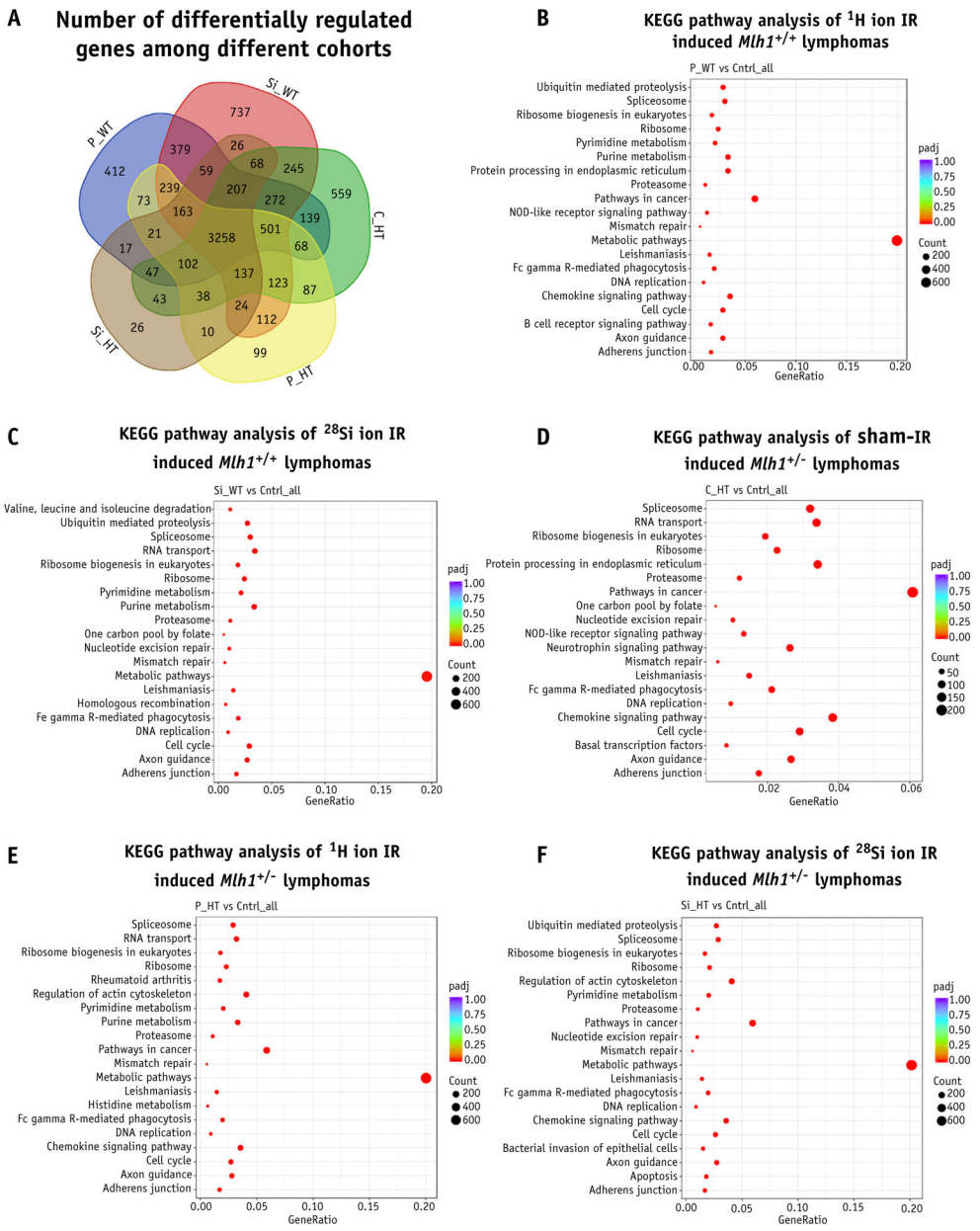

Fig. 4.

Gene ontology enrichment analysis of T-cell rich B-cell (TRB) lymphomas. (A) Venn diagram represents the number of differentially expressed genes among all *Mlh1* cohorts. KEGG pathway analysis represents the top 20 pathways involved in the process of lymphomagenesis of *Mlh1*$^{+/+}$ mice post (B) ^{1}H ion irradiation, and (C) ^{28}Si ion irradiation. KEGG (Kyoto Encyclopedia of Genes and Genomes) pathway analysis represents the top 20 pathways involved in the process of lymphomagenesis of *Mlh1*$^{+/-}$ mice post (D) sham irradiation (E) ^{1}H ion irradiation, and (F) ^{28}Si ion irradiation. *Abbreviations*: C_HT = sham irradiated *Mlh1*$^{+/-}$ cohort; Cntrl = control; IR = ionizing radiation; *P*_HT = ^{1}H ion irradiated *Mlh1*$^{+/-}$ cohort; *P*_WT = ^{1}H ion irradiated *Mlh1*$^{+/+}$ cohort; Si_HT = ^{28}Si ion irradiated *Mlh1*$^{+/-}$ cohort; Si_WT = ^{28}Si ion irradiated *Mlh1*$^{+/+}$ cohort.

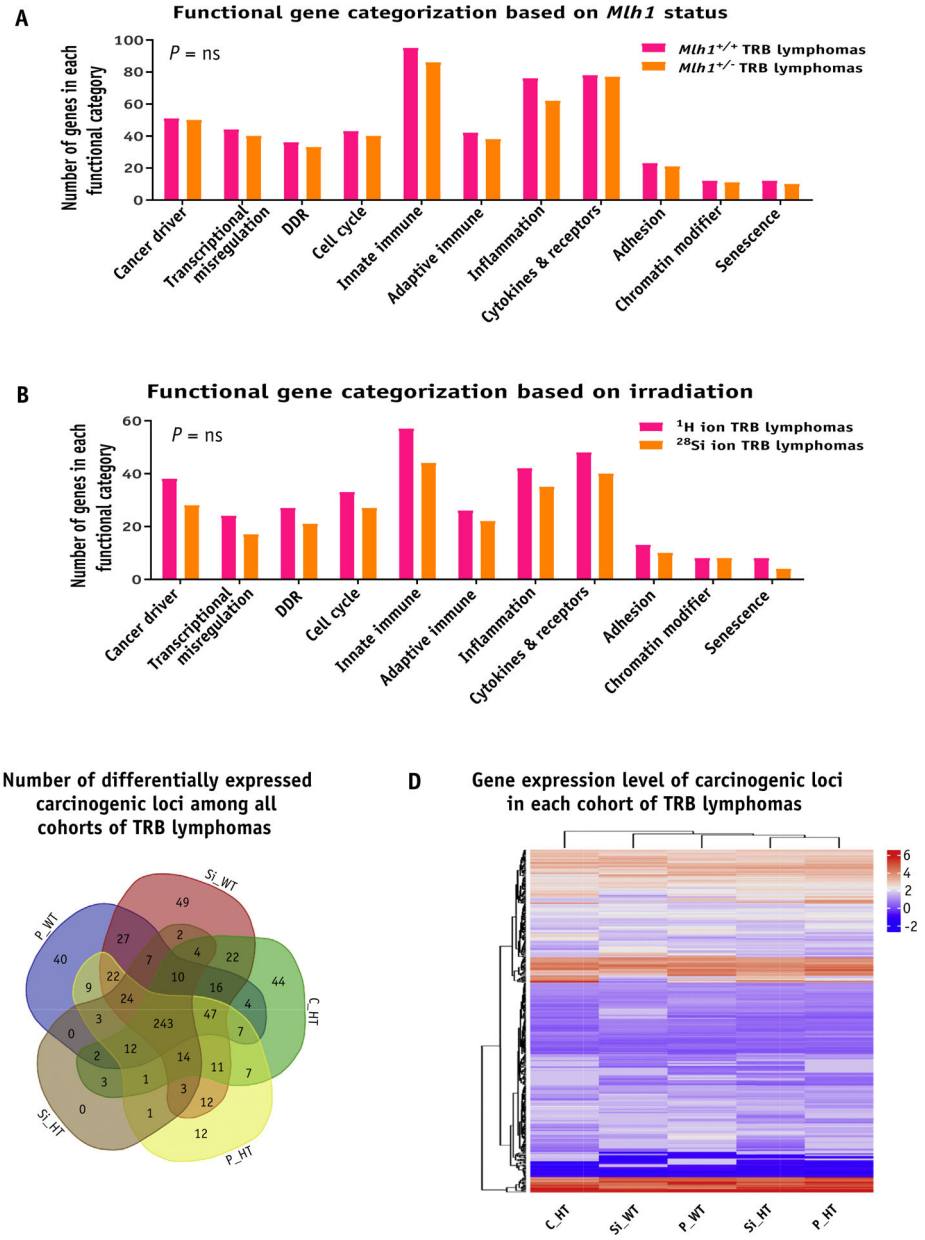

Fig. 5.

Gene expression analysis of T-cell rich B-cell (TRB) lymphomas. (A) The bar graph shows the number of genes that belong to each functional category when classified based on *Mlh1* status. (B) The bar graph shows the number of genes belonging to each functional category when classified based on irradiation source. (C) Venn diagram shows the number of differentially expressed carcinogenic loci among all cohorts of TRB lymphomas. (D) Heatmap represents the gene expression level of carcinogenic loci of each TRB lymphoma cohort in the form of hierarchical clustering. *Abbreviations*: C_HT = sham irradiated *Mlh1*$^{+/-}$ cohort; DDR = DNA damage response; ns = nonsignificant; *P*_HT = ^{1}H ion irradiated *Mlh1*$^{+/-}$ cohort; *P*_WT = ^{1}H ion irradiated *Mlh1*$^{+/+}$ cohort; Si_HT = ^{28}Si ion

irradiated *Mlh1*$^{+/-}$ cohort; Si_WT = ^{28}Si ion irradiated *Mlh1*$^{+/+}$ cohort; Cntrl = control. *P* values in bar graphs were determined by unpaired *t* tests.